NANOCRYSTAL SHAPE ANISOTROPY DETERMINATION USING EXAFS

© 2024   K. A. Svit[*], K. S. Zhuravlev

*Rzhanov institute of semiconductor physics, Siberian Branch of the Russian Academy of Sciences,
630090, Novosibirsk, Russia*

[*]*e-mail: svit@nanotech.nsk.ru*

Abstract. Using the set of the nanocrystals (NC) having the rectangular parallelepiped shape and a cubic crystal structure of the zinc-blende type as model system, the possibilities of determining the NC shape anisotropy using the polarized EXAFS technique were demonstrated. It was shown that the effective value of the coordination number of absorbing atoms in an NC with anisotropic shape depends on its size and the orientation of the X-ray radiation polarization vector relative to the NC surface. The effective values of the coordination numbers of the first coordination sphere of atoms in NCs having different size and surface composition were modeled. Taking into account the influence of the experimental error of the EXAFS method the possibilities of the model applicability for analysis of the real systems with NC were analyzed.

1. INTRODUCTION

Semiconductor nanocrystals (NC) are currently actively used to create optoelectronic devices (displays, solar cells, photodetectors, etc.) [1, 2]. This is due to the possibility of obtaining devices with greater efficiency and with better characteristics. For example, the use of NC in displays allows increasing the color gamut and reducing energy consumption. Recently, the possibility of creating LEDs based on NC with an external quantum yield was shown, more than 20% for red and green colors [3]. For practical application of optical devices based on NC, it is necessary to obtain a high quantum yield, which is determined by the ratio of the radiative and nonradiative exciton lifetimes. The radiative lifetime is determined by the fine structure of the exciton's basic state, which is caused by the splitting of the valence band as a result of spin-orbital interaction, as well as the influence of the exchange interaction of an electron and a hole, a crystalline field (for the case of a hexagonal lattice) and anisotropy of the NC shape. Moreover, it was shown that the tendency to splitting of the exciton energy levels due to the anisotropy of the NC shape is comparable to splitting due to the exchange interaction and the crystal field, which poses the task of determining the NC shape for an adequate analysis of their optical properties [4, 5].

The shape of NC is often evaluated by optical methods such as polarized absorption spectroscopy [5] and Raman spectroscopy [6]. The methods for determining the form of NC are based on the measurement of absorption and Raman scattering spectra at different sample orientations, relative to the polarization vector of electromagnetic radiation (parallel and perpendicular) and determining the size of the NC in different projections [7]. Currently, probe and electron microscopy methods are being actively used to obtain the most accurate information about the shape, size and structure of NC. However, their use in some situations is limited. Probe Microscopy methods do not allow determining the size and shape of NC enclosed in a matrix of another material. For these purposes, high-resolution electron microscopy (HREM) is used, which made it possible to determine the shape of various NC obtained by molecular beam epitaxy [8,9]. However, HREM also does not always allow us to study the form of NC due to the complexity of preparing samples [10]. For example, the problem of preparing samples for HREM in which NC are located in an organic
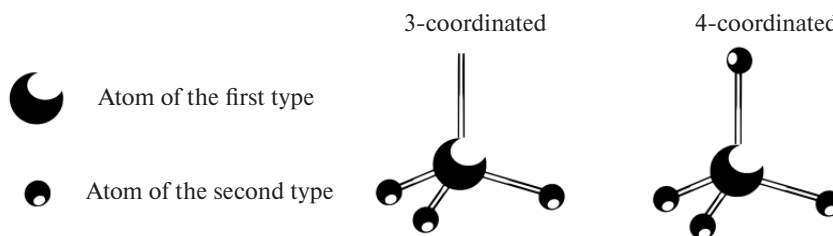
Fig. 1. Cd atoms surrounded by Se atoms. A fully coordinated cadmium atom (4c) is shown on the right, and a triple-coordinated Cd atom (3c) is shown on the left

matrix has not been solved. Therefore, the size and shape of NC synthesized in an anisotropic solid matrix of long organic molecules using Langmuir-Blodgett technology have not yet been determined [11].

Over the past decade, a method based on the analysis of the paired distribution function (PDF), which is a Fourier image from X-ray scattering data, has gained particular popularity in the study of the structure and shape of nanoscale materials [12, 13]. The PDF contains complete information about the structure of the nanomaterial, and therefore its shape. Determining the NC form from the experimental PDF by solving the inverse problem requires sorting through many different variants of model structures, which is quite labor-intensive. However, the development of computer technology, improvement of computational algorithms and many years of work by various research groups have led to the emergence of a number of ready-made solutions embedded in software packages for processing X-ray scattering data [14]. The proposed solutions make it possible to determine the shape and dimensions of the studied NC with comparatively high accuracy, and the PDF methodology itself is still developing and improving. Nevertheless, the PDF method is poorly suited for the study of low-concentration NC in the volume of the matrix due to the low signal-to-noise ratio. Moreover, the situation is particularly complicated for NC of small sizes (less than 5 nm in diameter) with a large size dispersion. This is due to the need to take into account the dependence of the disordered crystal structure of NC on its size [15].

More than 20 years ago, it was shown that the size of NC can be estimated from the fine structure of X-ray absorption spectra (EXAFS) [16]. EXAFS spectroscopy is a method of structural analysis and is used to obtain information about the atomic structure of a local atomic cluster

containing several coordination spheres near an atom excited by X- ray radiation. EXAFS spectroscopy allows determining the position of atoms, bond lengths, valence angles and parameters of thermal vibrations (the Debye-Waller factor). In comparison with the PDF, the EXAFS method has a higher sensitivity, since it is aimed at studying the local structure of a specific type of atoms. This method allows us to estimate the average size of the NC, using the effect of reducing the value of the effective coordination number with an increase in the ratio of the number of surface atoms to the total number of atoms in the NC [17]. Gregor and Lytle proposed a model for determining the shape of metallic NC according to the data EXAFS [18]. Their approach is based on the fact that the dependence of the value of the coordination numbers on the size of the NC differs for NC of different shapes. The model did not consider the structure of NC at the atomic level, and the formulas for the dependence of the coordination numbers on the number of atoms in the composition were derived from simple geometric considerations. This only allowed us to qualitatively describe the dependence of the fraction of surface atoms in different forms of NC. Subsequently, this approach was developed by Jantys, who also considered only metallic NC with a face-centered cubic lattice and proposed to determine the shape of NC from the ratio of coordination numbers for different coordination spheres [16].

However, the approaches described above have a number of limitations. With a relatively large size of NC (more than 200 atoms), differences in coordination numbers between NC of different shapes are comparable to the error of the EXAFS technique (about 10%), which makes these models difficult to apply to real systems where the dimensions NC is about 1000 atoms and more. The use of these NC models of semiconductor compounds (for example,

A2B6 or A3B5) is further complicated by the fact that they do not take into account the degree of enrichment of the NC surface by one or another element of the compound. In some cases, the solution of these problems is possible through the use of EXAFS polarizing spectroscopy. It is known that the spectrum EXAFS is sensitive to the orientation of the X-ray field vector $\mathbf{E}$ relative to the bonds directions in the crystal [19]. This leads to the fact that uncoordinated atoms on the NC surface give a different contribution to the ratio of coordination numbers at different orientations of the electric field vector $\mathbf{E}$. Since the number of uncoordinated atoms on the surface depends on the shape of the NC, it is possible to estimate the degree of anisotropy of the NC shape from a comparison of coordination numbers.

In this paper, we propose a technique for determining the anisotropy of the NC shape from polarized EXAFS spectra and apply it to NC with a cubic lattice of the zinc blende type, which is characteristic of NC based on a number of A2B6 and A3B5 semiconductors.

2. THE TECHNIQUE OF POLARIZED EXAFS SPECTROSCOPY

The oscillations in the EXAFS spectra are caused by the interference of the initial and scattered waves on the absorbing atom. To get information on the atomic structure of a local atomic cluster in the vicinity of several coordination spheres near an excited atom, the function $\chi(k)$ is determined from the EXAFS spectrum and compared with the calculation according to expressions (1) and (2):

$$\chi(k) = \sum_{i=1}^{\infty} A_i(k)\sin(2kR_i + \phi_i(k)), \qquad (1)$$

$$A_i(k) = \frac{N_i}{R_i^2 k} S_0 F_i(k)\exp(-2k^2\sigma^2)\exp(R_i\lambda_i), \qquad (2)$$

where $\phi_i(k)$ is an additional phase shift due to inelastic scattering, R_i is the distance to the i-th coordination sphere, $A_i(k)$ is the amplitude of the reflected wave, N_i is the coordination number of the i-th coordination sphere, S_0 is the coefficient of the EXAFS amplitude decay due to multielectronic effects, σ is the Debye–Waller factor, $F_i(k)$ is the amplitude of the backscattering of photoelectrons, λ is the free path of the photoelectron without loss of momentum. In this case, the parameters of the model are the number of atoms of the environment in the i-th coordination sphere, the radius in the i-th coordination sphere (the distance between atoms) of the atom, the Debye–Waller factor and the ionization energy.

An important feature is the high degree of linear polarization of X-ray synchrotron radiation. This allows us to characterize the material under study in different directions is due to changes in the angle between the X-ray polarization vector and the sample plane. For this purpose, the sample is exposed at different angles to the direction of the incident X-ray beam. The dependence on the direction of the polarization vector is most clearly manifested in the change in the coordination numbers of the first and second coordination spheres in crystal structures. The effective coordination number N_i for the i-th coordination sphere is expressed by the following formula:

$$N_i^* = 3\sum_{j=1}^{N_i}\cos^2(\alpha_j), \qquad (3)$$

where α_j is the angle between the vector of the electric field of incident X-ray radiation and the vector of the direction of the bond between the atom under study and the j-th atom in the i-th coordination sphere [16]. The accumulation occurs for all atoms in the i-th coordination sphere, the total number of which is N_i. In relation to the NC of binary semiconductor compounds with a cubic lattice of the zinc blend type let's consider a local atomic cluster in CdSe, one of the most popular materials for the synthesis of NC: a Cd atom with 4 Se atoms

According to formula (3) for a completely coordinated atom ($N_i = 4$), the coordination number of the first coordination sphere (N_1) can be expressed as

$$N_i^4 = 3\sum_{j=1}^{4}\cos^2(\alpha_j). \qquad (4)$$

For a fully coordinated atom, the coordination number does not depend on the direction of the vector $\mathbf{E}$ and is always 4. However, the situation changes for uncoordinated atoms, for example, surface ones. We will consider only triple-coordinated surface atoms (3c), since the formation of less coordinated atoms on the NC surface is less energetically favourable [20]. The value of N_1 for 3c depends on the orientation of the vector $\mathbf{E}$ due to the lack of one bond. The smallest value of N_1 (about 1) will be in the case when the vector $\mathbf{E}$ is parallel to the dangling bond, and, conversely, N_1 is the maximum (4) if the vector $\mathbf{E}$ is perpendicular to the dangling bond. Since the EXAFS signal is the sum of the signals from all absorbing atoms, the presence of surface atoms leads to a dependence of the shape of the total signal
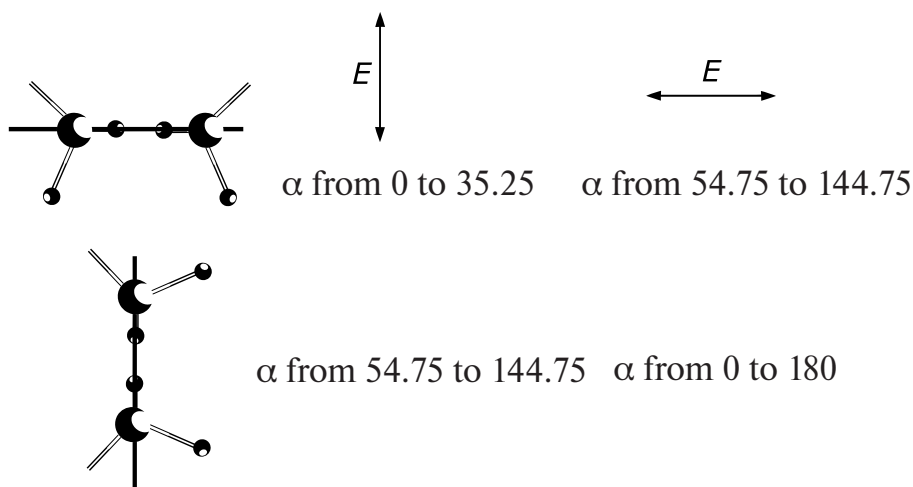
Fig. 2. A schematic representation of Cd atoms is shown from above on perpendicular, and below on parallel faces of NC to the vector *z*. For two directions of the vector (parallel and perpendicular to the *z* vector), the ranges of possible angles between the vector E and the broken bonds on the NC surface are represented

on the direction of the vector **E**. At the same time, the difference in the EXAFS signals measured at different orientations of the vector **E** will be the stronger the greater the ratio of the number of surface and volume atoms. Approximation of the EXAFS spectra by formulas (1) and (2) allows us to obtain effective values of the coordination numbers (N_{eff}), which are nothing more than the average value N_j for all absorbing atoms. However, the N_{eff} for NC will depend on the ratio of surface and bulk atoms, as well as the orientation of surface atoms relative to the polarization vector **E**.

3. THE MODEL

By analogy with the PDF method, obtaining information about the shape of NC from the dependence of the polarized EXAFS spectra on the angle between the vector **E** and the sample can be realized by solving the inverse problem using modeling of the studied structures and fitting the calculated spectra to experimental ones. Modeling EXAFS spectra with high accuracy implies knowledge of the positions of all absorbing atoms and atoms of their surroundings, and the experiment itself to obtain dependence of the EXAFS signal on the angle between the vector **E** and the sample requires many measurements, which is quite laborious. In addition, the contribution of the scattering atom to the EXAFS spectrum strongly attenuates when moving away from the absorbing atom, which makes it possible to obtain information only within several coordination spheres, which makes it possible to obtain information with high accuracy only about the local structure of the absorbing atom. For this reason, it is necessary to initially consider a more simplified approach from

which to judge on the possibilities of the methodology and the expediency of its further complication. We propose an approach based on comparing the coordination numbers of the first coordination sphere obtained from the analysis of EXAFS spectra measured at two (orthogonal) orientations of the vector **E**. This approach is relatively easy to implement, as it requires only two measurements. Since the synthesized NC differ in a variety of shapes and sizes, which are extremely difficult to model, let's consider a simple case of NC in the form of a straight-angle parallelepiped with a base of length L, width W and height H. This will simplify the modeling, but at the same time show the fundamental possibility of detecting anisotropy of the NC shape using EXAFS. Let us assume that NC does not contain bulk defects and has a cubic structure of the zinc blende type, which corresponds to the situation when the lengths of all bonds between the atoms of a binary compound are the same. In this case, we will consider the number of Cd atoms in one direction or another as a dimensional unit of length (regardless of their coordination number). In addition, assume that L = W, and H < L, W, in order to approximate as much as possible to the anisotropic spheroidal shape of real NC. Next, we consider the set of NC data of the same size, located in the volume of the matrix of another substance. Let's assume that the NC in the matrix are crystallographically disoriented relative to the **z** vector, but relative to the substrate they are oriented so that the height of the NC is parallel to the **z** vector. For convenience, we will specify the orientation of the vector **E** relative to the vector **z**. Initially, we assume that all atoms on the NC surface are Cd atoms. To determine the possible

values that the angle α can take between the polarization vector **E** and the dangling bonds on the NC surface, consider the NC surface in more detail. In Fig. 2 are schematically presented surface Cd atoms on faces perpendicular and parallel to the **z** vector.

Table 1. Average values of N_1 at different orientations of the vector **E**

Radiation polarization	Upper and lower faces	Side faces
$\parallel$	1.351	3.4
$\perp$	3.4	2.5

Ranges of α values can be found from simple geometric considerations, assuming that the angle between any of the two bonds of an atom in the state of sp^3 hybridization is 109.5°. For the case when the vector **E** is parallel to the vector **z** (parallel polarization), the range of α changes on the faces of the NC perpendicular to the vector **z**, ranges from 0 to 35.25° (the upper and lower faces are analogous, taking into account the periodicity of the sine function). For faces parallel to the **z** vector, α can have values from 54.75 to 144.75°. In the case when the vector **E** is perpendicular to the vector **z**, the ranges of α change. For the faces perpendicular to the **z** vector, the range of variation of α is from 54.75 to 144.75°. For faces parallel to the **z** vector, it is necessary to take into account that the NC can be rotated around the axis of symmetry parallel to the **z** vector at any angle. Therefore, α can be anything from 0 to 180°.

The determination of the average value of N_1 of the surface atom within the framework of the presented model can be obtained by integrating the expression (3) (N_i=3) over the entire range of α for a given atom and then dividing the result by the value of the range. Table 1 shows the average values of N_1 for atoms on the surface of the upper, lower and lateral faces of the NC with parallel and perpendicular orientation of the vector **E**.

When the value of N_1 for surface and bulk atoms is known, it remains to calculate the effective coordination number from the entire set NC, which, in turn, requires knowledge of the number of all types of atoms. Based on the dimensions of the parallelepiped, we calculated the number of volumetric and on top- the number of Cd atoms according to the following formulas:

$$S_{bulk} = (L-2)(W-2)(H-2), \qquad (5)$$

$$S_{vert} = 2LW, \qquad (6)$$

$$S_{side} = 4L(H-2), \qquad (7)$$

where S_{bulk}, S_{vert} and S_{side} are the number of bulk atoms, atoms on the upper, lower and side faces of the NC, respectively. The effective coordination number for the first coordination sphere from the entire NC group was calculated using the following formula.

$$N_{eff} = \frac{4S_{bulk} + S_{vert}N_{vert} + S_{side}N_{side}}{S_{bulk} + S_{vert} + S_{side}}, \qquad (8)$$

where N_{side} and N_{vert} are the average coordination numbers of the first coordination sphere for surface atoms on the lateral and vertical faces. We assume that the maximum size of NC is about 5 nm, which corresponds to about 30 Cd atoms in width and length of the base ($L = W = 30$). We introduce the concept of the anisotropy coefficient of the NC(C) shape as the ratio of its length to height $C = L/H$.

In order to understand how the difference in coordination numbers is related to the anisotropy of the NC shape, consider the ratio of effective coordination numbers with parallel and perpendicular orientations of vector **E** relative to vector **z** ($N_{eff\parallel} / N_{eff\perp}$). Figure 3 shows the data for calculating the dependence of on C for NC with different base sizes.
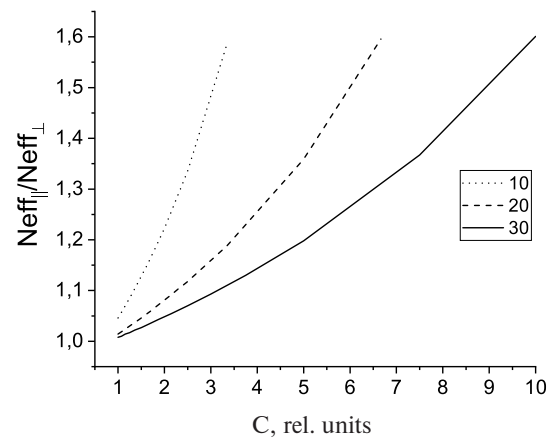

Fig. 3. The dependence of $N_{eff\parallel} / N_{eff\perp}$ on C for NC with different base sizes (L and W are 30, 20 and 10)
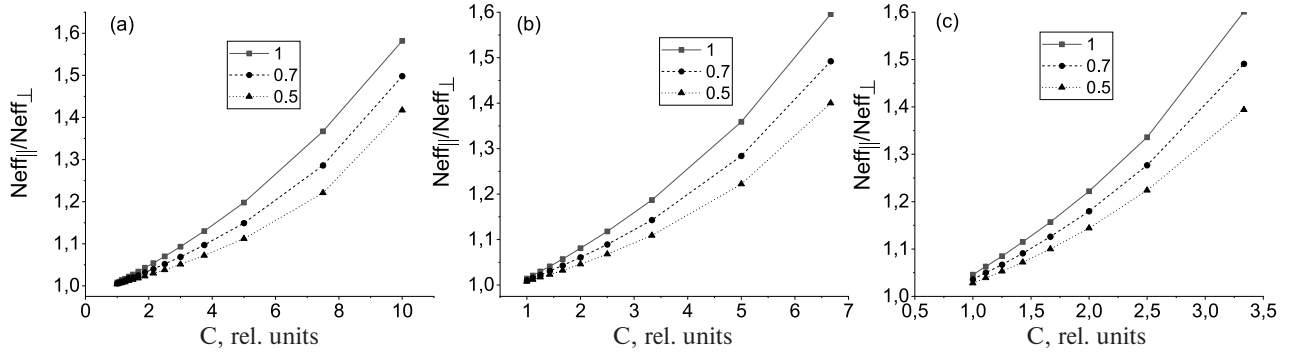
Fig. 4. Dependence of $N_{eff\|} / N_{eff\perp}$ on C for various θ_1: $L = W = 30$ (a), 20(b) and 10 (c). $\theta_1 = 1$ solid line (squares), $\theta_1 = 0.70$ dashed line (circles), $\theta_1 = 0.50$ dotted line (triangles)

It follows from the obtained dependences that $N_{eff\|} / N_{eff\perp}$ increases non-linearly with increasing C. However, the dependence is relatively weak, with increasing C by an order of magnitude, the value of $N_{eff\|} / N_{eff\perp}$ changes a little more than one and a half times. The dependence $N_{eff\|} / N_{eff\perp}$ changes a little more than one and a half times. The dependence of $N_{eff\|} / N_{eff\perp}$ on C becomes stronger with the decreasing lateral dimensions f the NC. The figure also shows that at C=1, when there is no anisotropy of the shape $N_{eff\|} / N_{eff\perp}$ does not equal to one and increases with decreasing the NC size. This is due to two features of the model that do not fully compensate for the difference in the values of $N_{eff\|}$ and $N_{eff\perp}$ when approximating the shape NC to cubic: (1) the number of surface atoms on the side faces is greater, since the number of side faces is twice as large; (2) Angle range for atoms on the side faces is additionally expanded due to the possibility of rotation of the NC around the axis of symmetry perpendicular to the plane of the substrate.

The presented calculations were carried out under the assumption that all surface atoms in the simulated NC are Cd atoms, which is not guaranteed in real systems. To account for the composition of the NC surface, we introduced a coefficient of Θ_1 equal to the proportion of cadmium atoms on the surface. Taking into account this coefficient, N_1 is expressed as

$$N_{eff} = \frac{4S_{bulk} + \dfrac{S_{vert}N_{vert}}{\Theta_1} + \dfrac{S_{side}N_{side}}{\Theta_1}}{S_{bulk} + \dfrac{S_{vert}}{\Theta_1} + \dfrac{S_{side}}{\Theta_1}}. \qquad (9)$$

Figure 4 shows the simulation data of the dependence of the value of $N_{eff\|} / N_{eff\perp}$ on C for NC, having different base sizes and surface composition. The lower value of θ_1 under consideration is 0.5 (half of the surface is covered with Cd atoms) and was chosen for the reasons that at a lower value, Se atoms should already be considered.

The figure shows that a decrease in the proportion of absorbing atoms on the surface of HC leads to the weakening of the dependence of $N_{eff\|} / N_{eff\perp}$ on C. The influence of the value θ_1 increases with increasing C, however, does not lead to a change in the value of $N_{eff\|} / N_{eff\perp}$ by more than 15%. Due to the fact that $N_{eff\|} / N_{eff\perp}$ depends on both θ_1 and the size of the crystal, the determination of one of these values requires knowledge of the other. Note that the value of Θ_1 can be determined independently by X-ray photoelectron spectroscopy, or set by the conditions of NC growth [21].

Let's consider the limits of applicability of the proposed methodology to the analysis of real systems. The model predicts that a cube-shaped NC has the value $N_{eff\|} / N_{eff\perp}$ more than one. Figure 5 *a* shows the calculated dependence of $N_{eff\|} / N_{eff\perp}$ on the size of the cube. It is clear that only if the experimental value of $N_{eff\|} / N_{eff\perp}$ is adjusted for the error of exceeding the values of $N_{eff\|} / N_{eff\perp}$ for a cube then the NC are anisotropic. The error of the Ni value obtained from the EXAFS spectra is usually in the range of 3% up to 10% [22,23], therefore, the error in determining $N_{eff\|} / N_{eff\perp}$ varies from 6 to 20%.

According to the dependencies shown in Fig. 3 and 5, with a known error value, it is possible to determine the minimum value of C for NC, at which the NC shape according to EXAFS data will be correctly defined as anisotropic. The minimum values of C are 1.25, 1.425 and 1.875 with an error of determining $N_{eff\|} / N_{eff\perp}$ 6% and 2, 2.5 and 3.75 with an error of 20% for NC with base sizes 10, 20 and
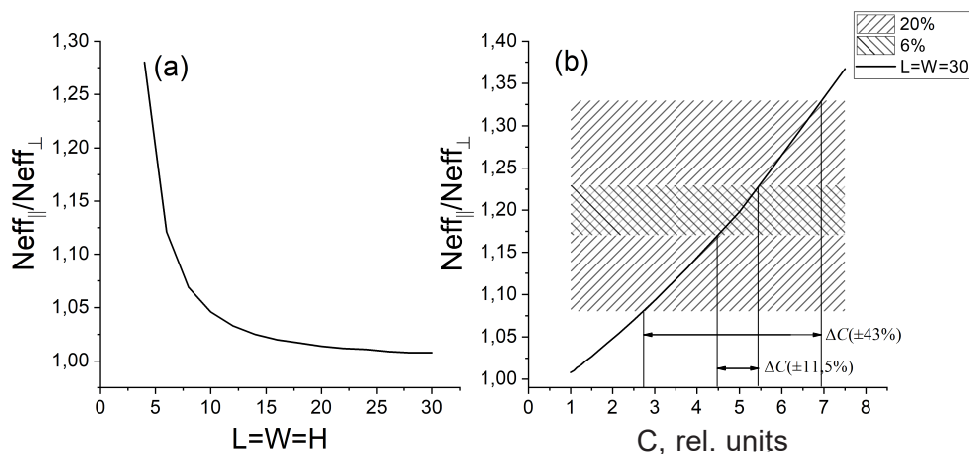
Fig. 5. a - Dependence of $N_{eff\parallel} / N_{eff\perp}$ for NC in the shape of a cube on the size. b - Dependence of $N_{eff\parallel} / N_{eff\perp}$ on C for NC with L = W = 30, the areas of experimental values of $N_{eff\parallel} / N_{eff\perp}$ are shaded (the average value is 1.2) taking into account the error of 6% (the slope of the strokes to the left) and 20% (the slope of the strokes to the right). The areas of experimental values intersect, which leads to the overlapping of strokes in the figure

30, respectively. It is obvious that the magnitude of the error also determines the accuracy of determining the value of C. Consider the case when the spread of the values of L, W and θ_1 it can be ignored. Figure 5b shows the dependence of $N_{eff\parallel} / N_{eff\perp}$ for NC with L = W = 30, and also shows, for example, the ranges of values of $N_{eff\parallel} / N_{eff\perp}$ (average value 1.2), taking into account the error is 6 and 20%. It can be seen that the errors in determining the value C (δC) are smaller the greater the slope of the $N_{eff\parallel} / N_{eff\perp}$C) curve, which is achieved with smaller lateral sizes of NC, greater values Θ_1 and C. To expand the possibilities of using the presented technique, it is necessary to increase the accuracy of the experiment, which is realized, in particular, by improving the quality of the preparation of samples, increasing their uniformity in thickness and composition.

4. CONCLUSION

The paper considers a technique for determining the anisotropy of the NC shape based on polarized EXAFS spectroscopy data. Application possibilities of the methodology were established using the simplified system consisting of a set of identical-sized NC in the form of a rectangular parallelepiped with a cubic crystal lattice of the zinc blende type. The principal possibility of using the technique of polarized EXAFS spectroscopy to obtain information about the anisotropy of the NC form was shown. The influence of the experimental error of the EXAFS technique on the limits of applicability of the proposed methodology is considered, in particular, the minimum values of the anisotropy coefficient are established, at which it is possible to qualitatively

establish that the NC are anisotropic in shape. It is shown that the sensitivity and accuracy of the technique increase with a decrease in the size of the studied NC. The values of the error in determining the value of the coefficient of anisotropy of the NC shape at various levels of experimental error of the EXAFS method are established.

An increase in the accuracy of the proposed technique is possible when it is used in conjunction with optical methods, microscopy methods and methods for determining the composition of the surface. The methodology itself can be useful for studying the form NC in organic matrices, where the preparation of the samples for HREM measurements is often difficult. Further development of the model consists in taking into account the spheroidal shape of the NC, as well as the variance of the NC in size.

REFERENCES

1. M. A. Cotta, ACS Appl. Nano Mater. 3, 4920 (2020).

2. D. S. Abramkin and V. V. Atuchin, Nanomaterials 12, 3794 (2022).

3. W. C. Chao, T. H. Chang, Y. C. Liu, Z. X. Huang, C. C. Liao, C. H. Chu, C. H. Wang, H. W. Tseng, W. Y. Hung, and P. T. Chou, Commun. Mater. 2, 96 (2021).

4. Al. L. Efros, M. Rosen, M. Kuno, M. Nirmal, D. J. Norris, and M. Bawendi, Phys. Rev. B 54, 4843 (1996).

5. E. S. Smotkin, C. Lee, A. J. Bard, A. Campion, M. A. Fox, T. E. Mallouk, S. E. Webber, and J. M. White, Chem. Phys. Lett. 152, 265 (1988).

6. J. J. Shiang, S. H. Risbud, and A. P. Alivisatos, J. Chem. Phys. 98, 8432 (1993).

7. P. Facci and M. P. Montana, Solid State Commun. 108, 5 (1998)

8. A. Aleksandrov, V. G. Mansurov, and K. S. Zhuravlev, Physica E 75, 309 (2016).

9. V. G. Mansurov, Yu. G. Galittsyn, A. Yu. Nikitin, K. S. Zhuravlev, and Ph. Vennegues, Phys. Stat. Sol. (c) 3, 1548 (2006).

10. S. Hovmoller, X. Zou, and T. E. Weirich, Adv. Imagin Electron Phys. 123, 257 (2002).

11. A. V. Nabok, A. K. Ray, and A. K. Hassan, J. Appl. Phys. 88, 1333 (2000).

12. T. M. Usher, D. Olds, J. Liku, and K. Page, Acta Cryst. A74, 322 (2018).

13. C. L. Farrow, C. Shi, P. Juhas, X. Peng, and S. J. L. Billinge, J. Appl. Crystallogr, 47, 561 (2014).

14. C. Shi, E. L. Redmond, A. Mazaheripour, P. Juhas, T. F. Fuller, and S. J. L. Billinge, J. Phys. Chem. C 117, 7226 (2013).

15. M. Khalkhali, Q. Liu, H. Zeng, and H. Zhang, Sci. Rep. 5, 14267 (2015).

16. A. Jentys, Phys. Chem. Chem. Phys. 1, 4059 (1999).

17. G. Agostini, A. Piovano, L. Bertinetti, R. Pellegrini, G. Leofanti, E. Groppo, and C. Lamberti, J. Phys. Chem. C 118, 4085, (2014).

18. R. B. Gregor and F. W. Lytle, J. Catal. 63, 476, (1980).

19. M. Shirai, T. Inoue, H. Onishi, K. Asakura, and Y. Iwasawa, J. Catal. 145, 159 (1994).

20. C. Giansante and I. Infante, J. Phys. Chem. Lett. 8, 8209 (2017).

21. C. J. P. Clark and W. R. Flavell, Chem. Rec. 18, 1 (2018).

22. N. S. Marinkovic, K. Sasaki, and R. R. Adzic, J. Electrochem. Soc. 165, J3222 (2018).

23. D. Kido and K. Asakura, Acc. Mater. Surf. Res. 5, 148 (2020)